Surface-plasmon resonance with infrared excitation: Studies of phospholipid membrane growth

Vladislav Lirtsman,[a] Roy Ziblat, Michael Golosovsky, and Dan Davidov
The Racah Institute of Physics, The Hebrew University of Jerusalem, Jerusalem 91904, Israel

Roman Pogreb
College of Judea & Samaria, Research Institute, Ariel, IL-44837, Israel

Vered Sacks-Granek and Judith Rishpon
Department of Molecular Microbiology and Biotechnology, Tel Aviv University, Tel Aviv 69978, Israel

(Received 4 May 2005; accepted 26 September 2005; published online 4 November 2005)

We report on a surface-plasmon resonance (SPR) technique based on a Fourier transform infrared spectrometer for biological and surface-sensitive applications. In contrast with conventional surface-plasmon techniques, which operate at a fixed wavelength and a variable angle of incidence, our setup allows independent variation of the wavelength and the angle of incidence. By the proper choice of these parameters, we achieve optimal coupling to the surface plasmon and high sensitivity. Moreover, by using infrared rather than visible light, we achieve an extremely narrow angular-dependent surface-plasmon resonance. This results in a very sensitive SPR technique that can easily sense one molecular layer. We take advantage of the extremely narrow SPR in the infrared range and use it to study the growth dynamics of the phospholipid layer, which is the main constituent of the biological cell membrane. In particular, we distinguish the difference in the growth dynamics of this artificial membrane from a solution under different conditions of liquid flow (continuous flow or injection). © *2005 American Institute of Physics*.
[DOI: 10.1063/1.2123370]

I. INTRODUCTION

A surface plasmon (SP) is an electromagnetic surface wave at the metal-dielectric interface. It is usually excited using a prism in the Kretschmann configuration.[1] The excitation of a surface plasmon occurs when the projection of a wave vector of the incident light k_x equals the SP wave vector k_{sp} (Fig. 1). In the attenuated total reflection regime this appears as a sharp reflectivity minimum which is usually measured by tracing the angular or wavelength dependence of the reflectivity. The position and width of this minimum are determined by the dielectric properties of the metal/dielectric interface. What makes the surface-plasmon technique so useful in thin-film studies is its utmost sensitivity to the presence of dielectric layers at the metallic surface.

In particular, this technique has been extensively used to study biological recognition[2–5] and the kinetics of film growth. Studying the liquids and soft matter using the surface-plasmon technique requires (1) the absence of moving parts and (2) a high sensitivity. An ingenious scheme for achieving this goal in the visible range was recently proposed in Ref. 6. However, the most natural way of achieving both these goals is to apply infrared frequencies using Fourier transform infrared (FTIR) spectrometer.

The infrared range offers several important advantages for using the surface-plasmon resonance (SPR) technique.

- A continuous source of infrared radiation is conveniently provided by the FTIR spectrometer.
- SPR-FTIR allows studying the wavelength-dependent reflectivity at a *fixed* incident angle. This results in more degrees of freedom for choosing the most sensitive configuration and is especially favorable for measuring the liquid samples.
- The width of the surface-plasmon resonance in infrared is extremely narrow.[3] This results in high sensitivity and better resolution in adsorption measurements.
- The infrared radiation, particularly in the 5–15 μm range, excites various vibrational/rotational modes in biological molecules, which may serve as "chemical fingerprints." That is why the infrared spectroscopy technique is so useful for organic chemistry and biology, where it allows one to differentiate between various substances. The surface-plasmon technique brings together all the advantages of infrared spectroscopy for studying very thin layers, including monolayers.[7]
- Being the bound wave, the surface plasmon decays exponentially away from the interface. Since the decay length in the direction perpendicular to the interface is on the order of the wavelength, the surface plasmon in the infrared range enables studying thicker layers. This is especially important for biologists, since most biological layers have a thickness of a few microns and cannot be easily studied using surface plasmon in the visible range.

Today, a few SPR studies in the infrared range use either a laser[2,8] or the FTIR spectrometer.[3] The SPR excitation and detection has been achieved using conventional technique based on a prism. Recently, the Coe and co-workers[7,9] sug-

[a]Author to whom correspondence should be addressed; FAX: 972-2-561-7805; electronic mail: lirtsman@vms.huji.ac.il

gested a nonconventional FTIR-SP technique based on the peculiar effect observed by Ebbesen *et al.*,[10] namely, surface-plasmon-mediated optical transmission through the periodic array of subwavelength-sized holes in the metallic layer. Here, we report on the more conventional SPR-FTIR technique that we use for studying the kinetics of the artificial cell membrane growth.

II. THE SPR-FTIR TECHNIQUE: THEORETICAL BACKGROUND

The surface plasmon is a surface electromagnetic wave propagating at the interface between two media with dielectric constants of opposite signs (see Fig. 1, upper panel). The real and imaginary parts of the surface-plasmon wave vector are as follows:[11]

$$k'_{sp} = \frac{\omega}{c}\sqrt{\frac{\varepsilon_2\varepsilon_3}{\varepsilon_2+\varepsilon_3}}, \tag{1}$$

$$k''_{sp} = \frac{\omega}{c}\sqrt[3]{\frac{\varepsilon_2\varepsilon_3}{\varepsilon_2+\varepsilon_3}}\frac{\varepsilon''_2}{2\varepsilon'^2_2}, \tag{2}$$

where $\varepsilon'_2<0$, $\varepsilon_3>0$. Note that $k'_{sp}>k_3$, where $k_3=(\omega/c)\sqrt{\varepsilon_3}$.

The most popular configuration for surface-plasmon excitation is the attenuated total reflection or so-called Kretschmann geometry.[1] This setup is based on a transparent prism with a dielectric constant ε_1. The base of this prism is coated by a thin metallic film with the dielectric constant $\varepsilon'_2+i\varepsilon''_2$, whereas $\varepsilon'_2<0$. This film is in contact with another dielectric having the dielectric constant ε_3. When the metallic film is sufficiently thin, the incident light beam excites the surface plasmon at the outer interface of the film. This excitation is resonant and occurs when the projection of the incident light wave vector on the interface equals the real part of the surface-lasmon wave vector [Eq. (1)], i.e., $k_1 \sin\theta = k'_{sp}$, where θ is the angle of incidence. By reverting this expression, we find the angle of the surface-plasmon excitation

$$\theta_{sp} = \sin^{-1}\left(\frac{k'_{sp}}{k_1}\right). \tag{3}$$

Since $k'_{sp}>k_3$, then $\theta_{sp}>\theta_{cr}$, where the critical angle θ_{cr} is $\theta_{cr}=\sin^{-1}(k_3/k_1)$. Using Eqs. (1) and (3) we obtain

$$\theta_{sp}-\theta_{cr} \approx \frac{k_3}{\sqrt{k_1^2-k_3^2}}\frac{\varepsilon_3}{2|\varepsilon'_2|}. \tag{4}$$

The angular width of the surface-plasmon resonance is determined by the imaginary part of the surface-plasmon wave vector. Equation (3) yields

$$\Delta\theta_{sp} = \frac{k''_{sp}}{\sqrt{k_1^2-k'^2_{sp}}}. \tag{5}$$

Using Eqs. (2) and (5) we obtain

$$\Delta\theta_{sp} \approx \frac{k_3}{\sqrt{k_1^2-k_3^2}}\frac{\varepsilon''_2}{2\varepsilon'^2_2}. \tag{6}$$

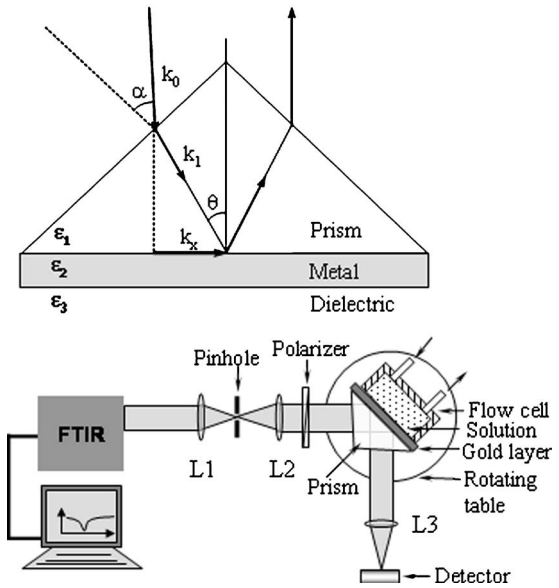

FIG. 1. Upper panel: the scheme of the surface-plasmon excitation. The arrows show the directions of the incident and the reflected beams. α is the the external angle of incidence and θ is the internal angle of incidence. The k_0 is the incident beam wave vector in vacuum, $k_1=k_0\,\varepsilon_1^{1/2}$ is the wave vector in the prism with the dielectric constant ε_1, and k_x is its projection on the glass-metal interface. Lower panel: SPR-FTIR experimental setup. A glass prism coated with a thin metallic (gold or silver) film is illuminated with a collimated, polarized beam from the FTIR spectrometer (Bruker Equinox 55). The reflected beam is detected with an InGaAs (D427) detector. The beam collimation is produced by a pair of BK-7 lenses L1 and L2 (with 62.9 and 150 mm focal lengths, respectively) and a 0.5 mm pinhole. A third BK-7 lens, L3 (D=25 mm, focal length 62.9 mm), focuses the beam into the detector. The sample (liquid in the flow cell or thin film) is in tight contact with the metallic substrate. The flow cell is mounted on the prism on a rotation stage.

In the following section we compare the surface plasmon in the visible and in the infrared ranges. We assume that ε_1, ε_3 are dispersionless and that the only parameter that changes with frequency is the dielectric constant of the metal, ε_2. The key issue here is that the real part of the dielectric constant of the metal is very high in the infrared range, $|\varepsilon'_2|\gg 1$, whereas in the visible range it is considerably smaller due to the proximity of the plasma edge, i.e., $|\varepsilon'_2| \geqslant 1$. This has two implications. First, the angle of the surface plasmon in the infrared approaches the critical angle, $\theta_{sp}-\theta_{cr}\sim 1/|\varepsilon'_2|$. Therefore, observation of the surface plasmon in the infrared range is more difficult than in the visible. However, this difficulty is counterweighted by the fact that the width of the surface-plasmon resonance in the infrared range is extremely narrow, $\Delta\theta_{sp}\sim 1/\varepsilon'^2_2$ [Eq. (6)]. Consequently, in practice, the angular resolution of the surface-plasmon technique in the infrared can be higher than that in the visible range. This is very important for accurate determination of the properties of thin dielectric layers deposited on the metal.

III. EXPERIMENTAL SETUP

Our experimental setup (Fig. 1, lower panel) is based on the prism in the Kretschmann configuration[3,11] and a Bruker Equinox 55 FTIR spectrometer as an infrared source. We introduced several computer-controlled stepping motors for

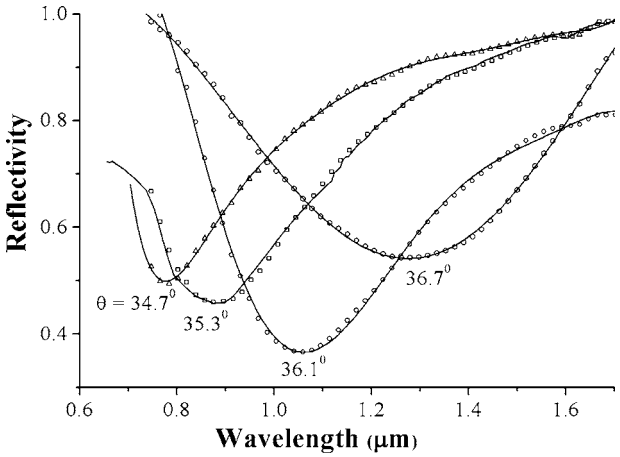

FIG. 2. A typical FTIR-SPR reflectivity vs wavelength for the Au/Air interface and for different angles of incidence θ. The solid lines represent the Fresnel prediction for the experimental data.

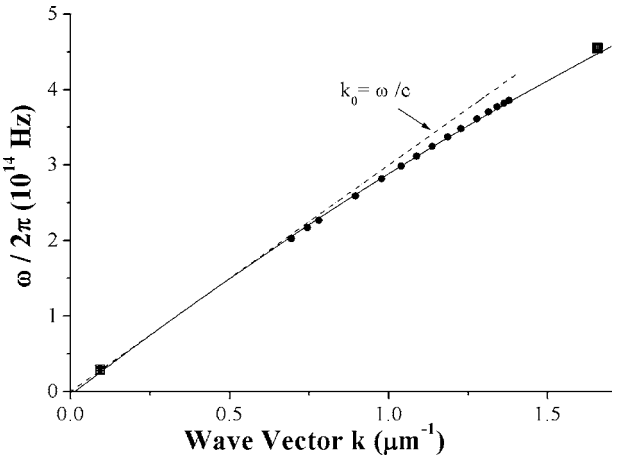

FIG. 3. Dispersion relation for the surface plasmons at the Au/air interface. The circles are experimental points. The solid line is a prediction of Eq. (2) using the dielectric constants of Refs. 13 and 14. The dashed line is the dispersion relation in air. The two extreme points (squares) in the figure were taken from the different SPR experiments using CO_2 ($\lambda=10.6$ μm) and HeNe ($\lambda=0.6328$ μm) laser excitations.

angular rotation and translation of the prism to allow measurements at varying wavelength and/or varying incident angle. Our present setup operates in the range of $0.75-2$ μm and includes a beam collimation system with a beam divergence of 0.23° and a beam diameter of 8 mm, an SF-11 glass right-angle prism, and a InGaAs (D427) mid-IR detector. The prism and detector are mounted onto a $\theta-2\theta$ rotation table with the angular precision of ±0.001°. The base of the prism is coated with a 30.4-nm-thick gold film using the electron-beam evaporation technique. This gold film thickness is optimal for the surface plasmon excitation in the $0.75-2$ μm wavelength range.

To study thin dielectric films, we deposited them onto a gold layer. To work with liquids, we use a special flow cell with two inlets whereby the liquid in the cell is in direct contact with the gold layer or with the insulating film deposited on it (Fig. 1, upper panel). The volume of the cell is 14 μL and its height is 200 μm. The flow system (Bioanalytical System, Inc.) includes a bee syringe pump with a variable speed controller. We used either (1) a "flow mode," namely, continuous flow of the solution through the cell during the SPR measurements; or (2) the "injection mode," namely, SPR studies after injection of a limited amount of the solution into the flow cell.

IV. EXPERIMENTAL PROCEDURE AND DATA ANALYSIS

For general characterization of the surface plasmon in the infrared range, we used the Au-coated prism without any dielectric layers on it. We measured reflectivity upon varying the wavelength λ at a fixed angle of incidence θ. All spectra were the average of 32 scans collected at 32 cm^{-1} resolution, corresponding to a wavelength step of ~5 nm. Figure 2 shows several experimental curves corresponding to different θ values. Each curve is characterized by a minimum in reflectivity whose position depends on θ. The solid lines are model predictions using the Fresnel reflectivity formulas[12] without any fitting parameters. These formulas take into account the refractive index of a glass prism,[13] the dielectric constant of gold,[14] and the gold film's thickness. The latter was determined using small-angle x-ray reflectivity studies.[15]

V. DISPERSION RELATIONS FOR THE SURFACE PLASMON IN THE INFRARED

We plotted the angular-dependent reflectivity for the Au-air interface for different wavelengths and determined dispersion relations for the surface plasmon at this interface. We identified the wavelength λ_{min} at the reflectivity minimum (Fig. 2), as that corresponding to the resonance excitation of the surface plasmon [Eq. (1)]. The λ_{min} yields the surface-plasmon frequency $\omega_{min}=2\pi c/\lambda_{min}$ whereas the θ yields the surface-plasmon wave vector [Eq. (3)]. By measuring the angular position of the reflectivity minimum at different wavelengths $\theta_{min}(\lambda)$ we obtain the dispersion relation $k_{sp}(\omega)$. Our experimental results (Fig. 3) are consistent with previous studies.[16] The solid line in Fig. 3 shows the model prediction for the Au-air interface using Eq. (1), $\varepsilon_3=1$ and $\varepsilon_2(\omega)$ from Refs. 13 and 14. At low frequencies, corresponding to the infrared range, the experimental data approach the dispersion in air (dashed line), whereas in the visible range, the data for the surface plasmon lie below the $k_0=\omega/c$ line, indicating the proximity to the plasma edge of the gold.

Importantly, our experiments show that the angular width of the surface-plasmon resonance in the infrared range is much narrower than the surface-plasmon resonance in the visible range, as predicted by Eq. (6). Indeed, Fig. 4 shows several angular dependencies of the reflectivity at different wavelengths. Two of these dependencies (at 1.4 and 1.2 μm) were obtained from vertical slices of the data plotted in Fig. 2. Two other curves (0.6328 and 10.6 μm) were obtained by measuring the angular dependence of the reflectivity at a constant wavelength using a HeNe laser and a CO_2 laser, correspondingly. Notably, there are very narrow resonances in the infrared range (especially at 10.6 μm) as compared to that in the visible (at 0.6328 μm). As shown in Fig. 5, the width of the surface-plasmon resonance increases with the wave vector and diverges at the plasma edge, as predicted by

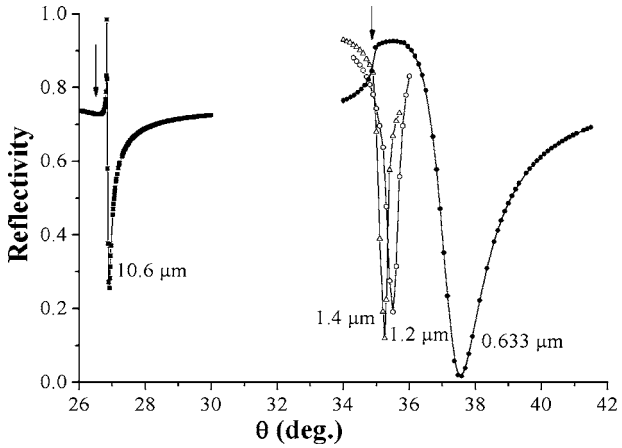

FIG. 4. Angular-dependent SPR. The data at 1.4 and 1.2 μm are extracted from Fig. 2. The data for 10.6 and 0.6328 μm show angular-dependent measurements using excitation from CO_2 and HeNe lasers, respectively. For the mid-IR we have used a special filter composed of two ZnSe lenses and a pin hole to decrease the beam divergence to 2 mrad or better. A gold film with a thickness of 9 nm was deposited directly on the base of the ZnSe right-angle prism. For the visible range we have used an SF-10 glass 60° prism and 47-nm-thick gold film. Vertical arrows indicate the critical angles of the prisms.

Eq. (6). Although the surface-plasmon resonance in the infrared is closer to the critical angle than in the visible range (compare the 10.6 and 0.6328 μm curves in Fig. 4), the resonance in the infrared range is much narrower.

VI. BIOLOGICAL APPLICATION: THE DYNAMICS OF HYBRID BILAYER MEMBRANE FORMATION

We used our highly sensitive infrared surface-plasmon technique to monitor the growth of the hybrid bilayer membrane from solution. Since this membrane cannot grow directly on the gold surface, we used an intermediate decanethiol monolayer. This layer is hydrophobic: it forms strong chemical bonding to gold and thus forms an interface between the gold and the phospholipid membrane. To form this intermediate layer, we injected 10 mM of the ethanolic solution of decanethiol into our flow cell and let it stay

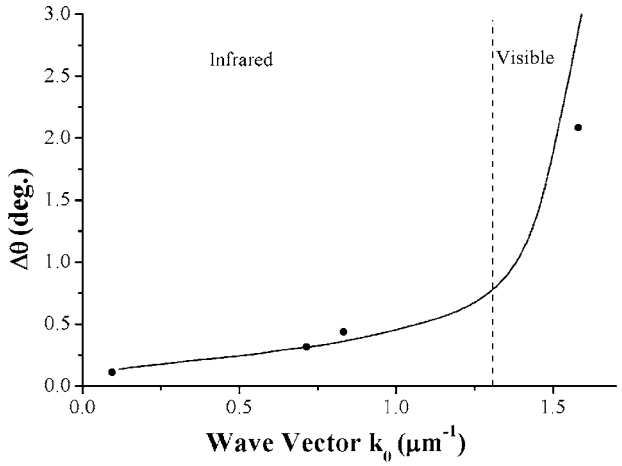

FIG. 5. Angular width of the SPR reflectivity minimum. Filled symbols show experimental data from Fig. 4. The solid line describes the imaginary part of the surface-plasmon wave vector k''_{sp}, as found from Eq. (2) and Ref. 14.

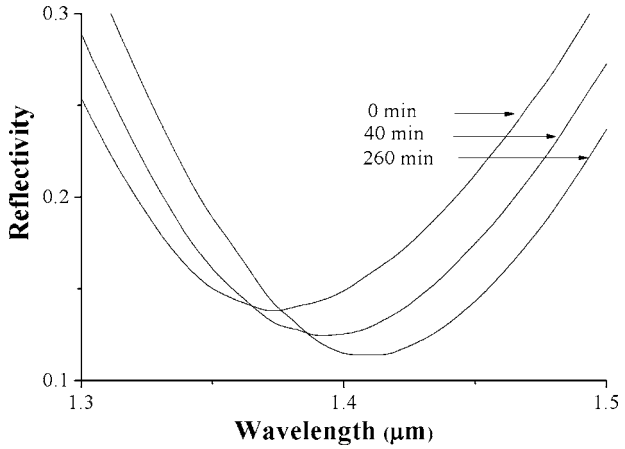

FIG. 6. FTIR-SPR minima at different growth stages of the decanethiol-phospholipid bilayer on thin gold film under the flow mode.

awhile. After 16 h the formation of decanethiol self-assembled monolayer was detected by the surface-plasmon technique, manifested as a redshift of the SPR minima (Fig. 2). Using Fresnel reflectivity formulas and a decanethiol refraction index[4] of 2.1, we found the decanethiol layer thickness $d_{dec}=0.95\pm0.5$ nm, as expected for a one molecular layer.[4,17]

To grow the membrane, we used a 20 mM ethanol solution of phospholipid 2-Oleoyl-1-palmitoyl-sn-glycero-3-phosphocholine(POPC). We added 0.2 mM of POPC solution to the phosphate buffer (NaCl—133 mM, K_2HPO_4—8.6 mM, KH_2PO_4—1.5 mM, pH=7.6). Since POPC tends to form vesicles, before each measurement we placed the solution in an ultrasonic bath for several minutes to split these vesicles.

Similar samples were prepared for the small-angle x-ray reflectivity studies.[18] Here, we covered glass slides with a Au/decanethiol layer and kept it in the shaking bath with the POPC solution for 5 h to form the membrane. The glass slide was air-dried and the x-ray measurements were performed. These measurements yielded a decanethiol thickness of $d_{dec}=0.95$ nm and a phospholipid layer thickness of $d_0=2.96\pm0.4$ nm. The d_0 value is consistent with the length of a POPC molecule as reported in Ref. 19.

For SPR measurements the POPC mixture was put into the flow cell (Fig. 1, lower panel). The phospholipid molecules adsorb on the decanethiol-modified gold surface and eventually form the continuous membrane. The kinetics of adsorption was monitored by the surface-plasmon technique. Two different experiments were conducted here: (a) adsorption under the flow rate of 2 μl/min (flow mode) and (b) adsorption without any flow (injection mode). In both cases the initial phospholipid concentration in solution was the same. As shown in Fig. 6, in the course of time the surface-plasmon resonance becomes progressively redshifted, indicating that adsorption took place. Figure 7 shows that the shift of the surface-plasmon resonance minima λ_{min} shifts with time and reaches saturation. In the flow mode the saturation occurs at $\Delta\lambda_{min}\sim50$ nm, whereas in the injection mode saturation is achieved at $\Delta\lambda_{min}\sim28$ nm.

Note two common properties of the membrane forma-

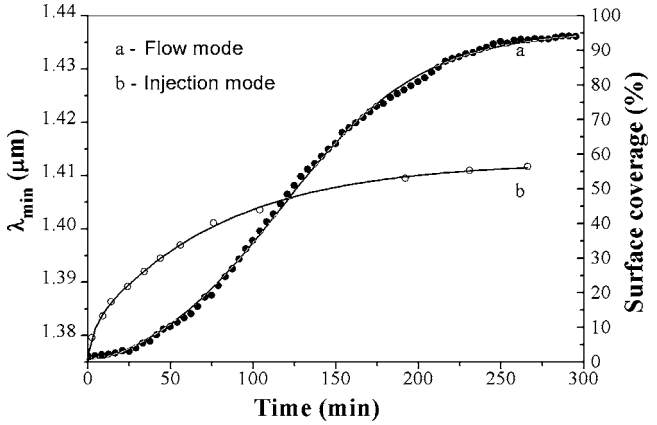

FIG. 7. SPR minimum vs time for POPC adsorption onto the gold-coated decanethiol monolayer for (a) flow mode and (b) injection mode. The solid line in (a) represents a stretched exponential fit: $P_{sat}[1-\exp(-t/\tau)^d]$, where $d=2.1$, $\tau=143$ min, and $P_{sat}=95\%$. The solid line in (b) is a fit for the Langmuir-type exponential behavior: $P_{sat}[1-\exp(-t/\tau)]$, where $P_{sat}=55\%$, $\tau=80$ min.

tion: (1) only one molecular layer of phospholipid can be formed and (2) the monolayer formation starts from small islands that then spread onto the surface. The surface-plasmon technique averages over the lateral structure of the layer. The length scale of the averaging is either the surface-plasmon propagation length or the beam size, whereas the islands are much smaller. Therefore, we relate the shift of the surface-plasmon resonance in Fig. 6 to the surface coverage P rather than to the film thickness (which nearly equals the length of the phospholipid molecule). We find the surface coverage $P(t)$ from the relation $P(t)=d_{\text{eff}}(t)/d_0$, where d_0 is the length of a single molecule; d_{eff} is derived from Fig. 6 and the Fresnel calculations, assuming that the dielectric constant of the monolayer equals its bulk value, $n=1.57$.

The results in Fig. 7 indicate the existence of different adsorption kinetics of phospholipid molecules onto the decanethiol-modified gold surface in the two different modes of the experiment. In the flow mode, $P(t)$ can be approximated by using a stretched exponential law:[20] $P=P_{sat}[1-\exp(-t/\tau)^d]$, where $P_{sat}=95\%$, $\tau=143$ min, $d=2.1$. The Langmuir exponent[21] yields a better expression for the injection mode, $P=P_{sat}[1-\exp(-t/\tau)]$. Here $P_{sat}=55\%$, $\tau=80$ min.

Because of the very narrow angular width of the surface-plasmon resonance in the infrared range, one usually observes two angular-resolved SPR peaks in inhomogeneous films of the phospholipid layer on the gold: one associated with the phospholipid on gold surface and another, associated with the free gold surface. The intensities of these peaks strongly depend on the adsorption time. Thus, surface coverage could be measured independently of the intensities of these resolved peaks.

VII. DISCUSSION

Why is there a pronounced difference between the membrane growth under the flow mode and under the injection mode? In the absence of flow (injection mode), the molecular motion in the solution is dominated by diffusion. Since the diffusion constant[22] for free lipid molecules is $D_{\text{free}}=20.5\ \mu\text{m}^2/\text{s}$, and the height of the cell is $h=200\ \mu$m, the diffusion time is $t\sim h^2/D_{\text{free}}=30$ min. This is compatible with the experimentally observed time constant in the injection mode. Note that the depletion of the solution after the membrane is grown, is non-negligible. Indeed, whereas the initial number of phospholipid molecules in the cell is 1.7×10^{15}, the complete coverage requires 1.5×10^{14} molecules. This number is calculated by dividing the cell area 72.4 mm^2 by the area for one molecule, 0.47 nm^2 (Ref. 19). Therefore, 10% of all molecules in solution are deposited. The linear time dependence of the surface coverage at the beginning of the process and the incomplete coverage at the saturation indicate that the membrane growth starts with small islands and that the resulting membrane is disordered. This is compatible with the previous studies.[21,23]

The phospholipid concentration in the solution under the flow mode is constant. Small phospholipid islands are "washed away" by the flow and only large islands remain. An induction period of ~20 min is needed to form these islands. However, the membrane grown from large islands is more perfect; hence the surface coverage under the flow mode is almost complete. The fit of the stretched exponential law in the flow case is consistent with previous papers[20] that assumed a "nonequilibrium" mechanism of adsorption induced by the flow.

VIII. CONCLUSIONS

We presented here a surface-plasmon technique based on the FTIR spectrometer. This technique allows SPR studies versus the wavelength and versus the incident angle. We demonstrated a very sharp surface-plasmon resonance in the IR range and provided a qualitative explanation for it. This very narrow resonance enables very high resolution and sensitivity as compared with SPR in the visible range. Together with the fitting procedure, it will be a very useful and sensitive tool for characterizing a wide range of thick organic and biological films.

We have used the FTIR-SPR technique to study molecular adsorption from the solution onto a gold-coated surface. Importantly, we demonstrated that the adsorption mechanism strongly depends on the growth conditions. Under flow conditions, the surface coverage is more homogeneous than in the absence of flow. In the latter case the surface coverage is only partial, probably due to disorder and the formation of small islands.

ACKNOWLEDGMENTS

This work was supported by the Israeli Ministry of Science. We are grateful to the late Dr. Mark Levin for his help in system design during the initial stages of this research. One of the authors (D.D.) would like to acknowledge helpful correspondence with J. R. Sambles concerning SPR in the infrared range.

[1] E. Z. Kretschmann, Z. Phys. **241**, 313 (1971).
[2] G. Brink, H. Sigl, and E. Sackmann, Sens. Actuators B **25**, 756 (1995).
[3] A. G. Frutos, S. C. Weibel, and R. M. Corn, Anal. Chem. **71**, 3935 (1999).
[4] A. L. Plant, M. Brighamburke, E. C. Petrella *et al.*, Anal. Biochem. **226**,

342 (1995).
[5]E. Kaganer, R. Pogreb, D. Davidov *et al.*, Langmuir **15**, 3920 (1999).
[6]I. R. Hooper and J. R. Sambles, J. Appl. Phys. **96**, 3004 (2004).
[7]K. R. Rodriguez, S. Shah, S. M. Williams, and J. V. Coe, J. Chem. Phys. **121**, 8671 (2004).
[8]E. V. Alieva, Y. E. Petrov, and V. A. Yakovlev, Opt. Spectrosc. **86**, 740 (1999).
[9]S. M. Williams, K. R. Rodriguez, S. Teeters-Kennedy, A. D. Stafford, S. R. Bishop, U. K. Lincoln, and J. V. Coe, J. Phys. Chem. B **108**, 11833 (2004).
[10]T. W. Ebbesen, H. J. Lezec, H. F. Ghaemi *et al.*, Nature (London) **391**, 667 (1998).
[11]H. Raether, Springer Tracts Mod. Phys. **111**, 1 (1988).
[12]D. L. Windt, Comput. Phys. **12**, 360 (1998); M. Born and E. Wolf, *Principles of Optics: Electromagnetic Theory of Propagation, Interference and Diffraction of Light*, 6th ed. (Oxford, New York/Pergamon, New York, 1980).
[13]Schott Glaswerke (SCHOTT Optisches Glas, Germany, Mainz, 1992).
[14]E. D. Palik, *Handbook of Optical Constants of Solids* (Academic, New York, 1985).
[15]M. Tarabia, H. Hong, D. Davidov *et al.*, J. Appl. Phys. **83**, 725 (1998).
[16]R. Ruppin, Solid State Commun. **8**, 1129 (1970); N. Marschall, B. Fischer, and H. J. Queisser, Phys. Rev. Lett. **27**, 95 (1971).
[17]V. Chechik, H. Schonherr, G. J. Vancso *et al.*, Langmuir **14**, 3003 (1998).
[18]The x-ray source for this experiments was a Rigaku rotating anode Cu source operated at 12 kW with a double Ge monochromator to eliminate $K\alpha$ radiation, yielding $\lambda = 1.5418$ Å. Three sets of Huber slits produced an in-plane resolution of 0.02 $Å^{-1}$. Data were collected using $\theta - 2\theta$ scans with a PMT tube and NaI scintillator. Background was obtained from the x-ray glass slide covered by 290 Å Au film. For reflectivity calculations we used the "PARRATT32" program (HMI, Berlin Neutron Scattering Center).
[19]S. Tristram-Nagle, Y. Liu, J. Legleiter *et al.*, Biophys. J. **83**, 3324 (2002).
[20]A. T. A. Jenkins, R. J. Bushby, S. D. Evans *et al.*, Langmuir **18**, 3176 (2002); Y. F. Chen, Phys. Rev. B **40**, 3437 (1989).
[21]T. Neumann, M. L. Johansson, D. Kambhampati *et al.*, Adv. Funct. Mater. **12**, 575 (2002); Y. E. Lozovik, and A. M. Popov, Surf. Sci. **414**, 57 (1998).
[22]A. Sonnleitner, G. J. Schutz, and T. Schmidt, Biophys. J. **77**, 2638 (1999).
[23]S. Haemers, G. J. M. Koper, M. C. van der Leeden *et al.*, Langmuir **18**, 2069 (2002).